Wasp-inspired needle insertion with low net push force

Sprang, Tim; Breedveld, Paul; Dodou, Dimitra

DOI
10.1007/978-3-319-42417-0_28

Publication date
2016

Document Version
Accepted author manuscript

Published in
Biomimetic and Biohybrid Systems

Citation (APA)
Sprang, T., Breedveld, P., & Dodou, D. (2016). Wasp-inspired needle insertion with low net push force. In N. F. Lepora, A. Mura, M. Mangan, P. F. M. J. Verschure, M. Desmulliez, & T. J. Prescott (Eds.), *Biomimetic and Biohybrid Systems: Proceedings of the 5th International Conference Living Machines 2016* (pp. 307-318). (Lecture Notes in Computer Science (including subseries Lecture Notes in Artificial Intelligence and Lecture Notes in Bioinformatics); Vol. 9793). Springer. https://doi.org/10.1007/978-3-319-42417-0_28

Wasp-inspired needle insertion with low net push force[1]

Tim Sprang, Paul Breedveld, and Dimitra Dodou

Department of BioMechanical Engineering, Faculty of Mechanical, Maritime and Materials Engineering, Delft University of Technology, Delft, The Netherlands
d.dodou@tudelft.nl

Abstract. This paper outlines the development of a four-part needle prototype inspired by the ovipositor of parasitic wasps. In the wasp ovipositor, three longitudinal segments called valves move reciprocally to gain depth in the substrate. It has been suggested that serrations located along the wasp ovipositor induce a friction difference between moving and anchoring valves that is needed for this reciprocal motion. Such an anchoring mechanism may not be desired in a medical setting, as serrations can induce tissue damage. Our aim was to investigate whether a multipart needle can penetrate tissue phantom material with near-zero net push force while using needle parts devoid of surface gripping textures or serrations. Accordingly, a four-part needle prototype was developed and tested in gelatine substrates. The performance of the prototype was assessed in terms of the degree of slipping of the needle with respect to the gelatine, with less slip implying better performance. Slip decreased with decreasing gelatine concentration and increasing offset between the needle parts. Motion through gelatine was achieved with a maximum push force of 0.035 N. This study indicates the possibility of needle propagation into a substrate with low net push force and without the need of serrations on the needle surface.

Keywords: Percutaneous interventions, Wasp ovipositor, Biomimetics

1 Introduction

1.1 Percutaneous needles: a brief state-of-the-art

Blood sampling, biopsies, regional anaesthesia, neurosurgery, and brachytherapy, all rely on percutaneous needles [1]. Most needles used in these procedures are rigid and follow straight trajectories. Accessibility of targets located deep inside the body is inhibited, and deviations from the desired path due to organ deformation are common [2]. These functional limitations hamper medical treatment when designated areas cannot be reached [2] and compromise safety when undesired areas are penetrated [3].

[1] *This is an Author's Accepted Manuscript of an article published in Lecture Notes in Artificial Intelligence [copyright Springer]*. Sprang, T., Breedveld, P., & Dodou, D. (2016). Wasp-inspired needle insertion with low net push force. In N. F. Lepora, A. Mura, M. Mangan, P. F. M. J. Verschure, M. Desmulliez, & T. J. Prescott (Eds.), *Living Machines 2016, Lecture Notes in Artificial Intelligence, 9793*, 307–318. doi: 10.1007/978-3-319-42417-0_28

Several flexible steerable needles have been developed in an effort to overcome the path planning limitations encountered with rigid straight needles (e.g., [2],[4–9]). Some of these newly developed needles rely on concentric axial insertion of multiple pre-bent needle parts, whereas others rely on reaction forces from the tissue to control the steering curvature (for reviews see [10,11]). One drawback of flexible needles is that the axial load applied at the back of a needle increases with resistive forces on the needle tip and shaft when penetrating deeper into the tissue. The tissue can only support this axial load up to a certain penetration depth; further needle advancement can lead to buckling of the needle and/or lateral slicing and damage of the tissue.

1.2 The wasp ovipositor and biologically inspired steerable needles

The wasp ovipositor is a needle-like structure, with no musculature. The ovipositor extends from the last abdominal segments of the wasp and serves the main purpose of egg deposition. The ovipositor consists of three longitudinal segments called valves: two ventral valves and one dorsal valve. The dorsal valve is connected to the two ventral valves along its length by means of a tongue-and-groove mechanism that allows for relative movement of the valves in the direction of the ovipositor while preventing their separation. Abdominal musculature actuates the valves independently from each other [12,13]. The wasp penetrates the substrate by antagonistically moving the ventral valves while the dorsal valve acts as sliding support. Serrations at the ovipositor tip are likely to allow the valves anchor against the substrate (**Fig. 1**). It has been hypothesized that the wasp applies a pull force on the anchored valve, allowing to load the penetrating valve with a push force higher than its critical buckling load [14,15].

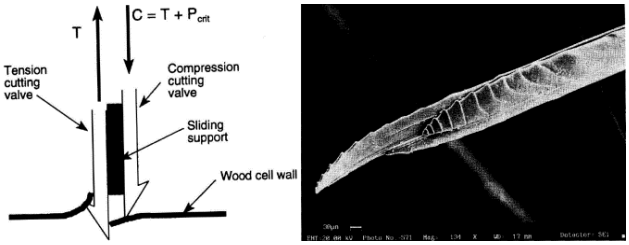

Fig. 1. Schematic representation of the hypothesized working principle of penetration of a wasp ovipositor (left). The SEM image (right) shows the tip of the ovipositor of *Megarhyssa nortoni nortoni*, an Ichneumonoid parasitoid wasp (figures from [14]).

The wasp ovipositor has been used as an inspiration source for designing steerable percutaneous needles [3],[15–19]. For example, Oldfield et al. [18] described a 6-mm diameter four-part needle prototype with reciprocally moving segments. Tissue transversal with no net axial force by means of microstructures on the needle surface has been reported in [6],[16],[19]. Similarly, inspired by insertion methods observed in mosquito proboscis, Aoyagi et al. [20] indicated that substrate penetration with a mi-

croneedle comprising serrated stylets is possible without applying a net push force (see also [21] for a description of buckling prevention in mosquitos and wasps).

1.3 Goal of this study

It has been suggested that the serrations located on the wasp ovipositor induce a friction difference between moving and anchoring valves [19]. Serrations may not be desired in medical settings, as they can induce tissue damage. Our aim was to investigate whether a multipart needle can penetrate tissue phantom material with low net push force while being devoid of any surface gripping textures or serrations.

2 Design of a multipart needle prototype

A multipart needle prototype was developed, comprising a low-friction cart that suspended a four-part needle assembly, four linear actuators, and driving electronics to move a needle assembly back and forth (**Fig. 2**). The needle assembly consisted of four stainless steel square needle parts and a stainless steel guide tube. The needle assembly had a total diameter of 2 mm (cf. diameter range of common hypodermic needles: 0.2–4.3 mm [22]) and a length of 200 mm (in line with the penetration depths in [6]). The needle tip was conical (angle about 20^{o}) and sharp. The needle parts had a smooth surface finish (R_a = 0.2); here we differentiate from [19] where saw-tooth microstructures were used to induce friction.

Each needle part ended in a fin mounted to a leadscrew, each leadscrew being translated back and forth by a linear stepper motor (resolution: 1.8^{o}, corresponding to 0.0061 mm/step of leadscrew translation). The motors were mounted in an aluminium bracket. Two alignment pins, extending from the bottom of the bracket, aligned the needle and actuator assembly with the low-friction cart. The cart was supported by two axes, each containing two ball bearings with metal shields (624-ZZ, 4x13x5 mm).

Four stepper drivers were mounted behind the linear actuator module. The drivers were controlled with a microcontroller. A two-row LCD display showed a timer and cycle counter during actuation, and settings when standby. The settings were controlled by two push buttons and a rotary encoder. The system was battery powered.

The embedded code was written in C++ including Arduino libraries. The software consisted of a user interface part containing a rotational encoder with a push button, a green button, a red button, and the display driver, and an embedded part containing the register, stepper sequence controller, stepper controller, and stepper driver.

Needle penetration was realized in cycles, each of which consisted of a protrusion and a retraction phase. In the protrusion phase the needle parts were protruded one-by-one (or two-by-two, depending on the sequence setting) with respect to the cart over a distance equal to a predefined offset. In the retraction phase the needle parts were retracted altogether with respect to the cart, over a distance equal to the offset.

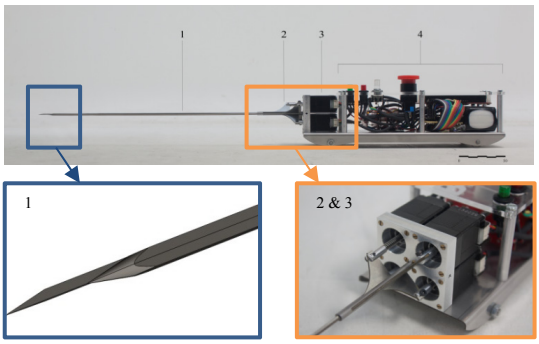

Fig. 2. Image of the prototype, showing the needle (1), needle assembly (2), linear actuator assembly (3), and the low friction cart with driving electronics (4).

3 Hypotheses

In a four-part needle, zero net push force penetration relying on a friction difference due to a difference between the number of stationary and protruding needle parts would require the advancement of one needle part at a time. Previous measurements in porcine liver showed that friction force on a needle with a diameter of 1.27 mm increased linearly with penetration depth, whereas cutting forces remained about constant along the penetration depth [23,24]. It can be therefore expected that, when protruding one needle part at a time, an equilibrium between the friction force on the stationary needle parts and the resistive force (i.e., sum of cutting force F_c and friction force F_f) on the protruding needle part is reached at a certain penetration depth:

$$\left(\frac{1}{4}F_c+\frac{1}{4}F_f\right)_{protruding}=\left(\frac{3}{4}F_f\right)_{stationary} \tag{1}$$

From this depth onwards, penetration with zero net push force is theoretically possible, since the friction force on the stationary needle parts is higher than the resistive force on the protruding needle part.

The performance of the prototype was assessed in terms of the degree of slipping of the needle with respect to the gelatine, with less slip implying better performance. The following hypotheses were investigated:

- *Protrusion sequence:* When moving one needle part at the time, performance is not expected to be affected by the protrusion sequence, as the surface area difference between moving and stationary needle parts is independent from the protrusion sequence. A two-by-two actuation is expected to result in no penetration, as in that case the friction force on the stationary needle parts is smaller than the resistive forces on the protruding needle parts.

- *Needle-part velocity:* Friction force increases with insertion velocity more steeply than the corresponding cutting force [25]. Following Eq. 1, it is thus expected that the needle performs better at higher velocities.
- *Gelatine concentration:* In very low gelatine concentrations no penetration is expected, as there is no sufficient needle-substrate friction to overcome the bearing friction and inertia of the car. Resistive forces on the protruding needle parts are likely to also be dominant in high concentrations, leading to poor performance. An optimum in gelatine concentration is thus expected for best performance.
- *Offset:* The friction force on the protruding needle part is expected to be higher for a larger offset, due to the larger surface area compared to the area for lower offsets.

4 Methods

Two experiments were conducted. In the first experiment (called henceforth prototype experiment), the effect of gelatine concentration, needle-part offset, needle-part velocity, and needle-part sequence on the performance of the prototype was measured. In the second experiment (force experiment), force measurements were conducted during the insertion of the needle into gelatine to estimate the relation between cutting and friction force as a function of needle velocity and gelatine concentration.

4.1 Experimental setup

Prototype experiment. A platform consisting of an aluminium frame and a 500x500x8 mm acrylic plate formed a level surface for the low-friction cart to travel back and forth between a proximity sensor and a gelatine sample. Adjustment screws ran through rivet nuts on the four corners of the frame for levelling. Gelatine substrates were produced in 434x344x107-mm trays. One panel of each tray had a 20x2 grid of 15-mm diameter holes, each 40 mm apart. The tray was set to height with spacers, and oriented so that the panel with holes was positioned against the platform. A laser proximity sensor (Micro-Epsilon optoNCDT1302-200; range: 200 mm; resolution: 0.1 mm) measured the travelled distance of the prototype. The sensor was mounted on a bracket and placed against the platform to ensure a constant distance between the sensor and gelatine tray. Sensor data were sampled at 50 Hz using LabVIEW 2010 and a National Instruments NI USB-6210 16-bit data acquisition system.

Force experiment. The four needle parts and guide tube were clamped to a force sensor assembly with the tip directed downwards. The needle was translated by means of a linear stage. The axial force was measured during the insertion and retraction movement of the needle in a gelatine container positioned underneath the needle. The force sensor assembly consisted of a mechanical decoupler holding a force transducer. The sampling rate was set at 1 kHz. The decoupler assembly was statically calibrated with balance weights ranging between 0.25 and 1.0 kg in steps of 0.25 kg.

4.2 Variables

Independent variables. The following variables were manipulated:

- *Needle-part offset* [mm]: The length of the protruding part of the moving needle parts relative to the stationary needle parts varied between 3, 10, and 20 mm.
- *Needle-part velocity* [mm/s]: The protrusion and retraction velocity of the needle parts with respect to the cart, varied between 4, 8, and 13.5 mm/s, where 13.5 mm/s is the maximum velocity that the linear actuators were able to generate.
- *Gelatine concentration* [% wt]: The % weight of gelatine powder in water, varied between 3, 8, and 13% wt, to simulate a variety of soft tissues, from brain and fat to breast and liver tissue [26,27].
- *Needle-part sequence* [no units]: The sequence of protruding needle parts, varied between circular, diagonal, and a two-by-two manner of actuation.

Dependent variables (measured). The following variables were measured:

- S_a [mm]: The distance travelled by the cart (prototype experiment).
- *Number of cycles* (N_c) [no units]: The number of cycles performed by the cart to travel a given distance (prototype experiment).
- F_i [N]: The axial force acting on the needle during insertion, measured with the force transducer. F_i represents the sum of the needle cutting force and the needle-substrate friction force (force experiment).
- F_f [N]: The axial force acting on the needle during retraction. F_f represents the needle-substrate friction force (force experiment).

Dependent variables (derived). The following variables were calculated:

- S_t [mm]: The number of cycles multiplied by the offset representing the theoretical distance that the cart would travel if there were zero slip (prototype experiment).
- $Slip_{pro}$ [mm]: The slip during protrusion, equalling the backwards travelled distance of the cart during the protrusion of the needle in one cycle (prototype experiment).
- $Slip_{ret}$ [mm]: The slip during retraction, equalling the difference between the offset and the actual travelled distance of the cart during retraction (prototype experiment).
- SR_{tot} [no units]: The slip ratio over an entire measurement, defined as $SR_{tot} = 1 - S_a/S_t$. Less slip means less dependence of the needle penetration on the net axial push force on the needle (prototype experiment).
- SR_{pro} [no units]: The slip ratio in the protrusion phase, defined as: $SR_{pro} = Slip_{pro}/Offset$ (prototype experiment).
- SR_{ret} [no units]: The slip ratio in the retraction phase, defined as: $SR_{ret} = Slip_{ret}/Offset$ (prototype experiment).
- F_c [N]: The cutting force defined as the axial force on the needle as a result of the subtraction of the retraction force from the insertion force (force experiment).
- *Depth of equilibrium* [mm]: The depth at which F_c and F_f are in equilibrium according to Eq. 1 (force experiment).

4.3 Experimental procedure

Prototype experiment. Gelatine was prepared in trays one day in advance of the experiment. The needle was positioned in front of the allocated hole of the tray and a machinist square was used to align the cart perpendicular to the platform. Before the start of each measurement, the needle was manually pushed 35 mm into the gelatine (this initial depth was defined in pilot measurements as the minimum distance for which needle advancement was possible; for smaller distances, the contact area of the needle with the gel was not sufficient and the needle slipped instead of advancing). Next, the proximity sensor was placed against the base of the platform, aligned with the cart, and switched on. About 1 s later, the actuation of the needle parts started and continued until the needle had travelled about 120 mm inside the gelatine.

All measurements were performed over a time span of one day. The four independent variables were varied from a common baseline, see **Table 1**. Measurements were repeated five times for each combination of parameters. Measurement allocation to the tray holes was done quasi-randomly, so that each set of five measurements in 8% wt gelatine was distributed over the upper and lower rows of three trays. All measurements in 3% wt and 13% wt gelatine were performed in a single tray and distributed randomly between the upper and lower rows of the tray.

Table 1. Parameter variation in prototype experiment.

Sequence [no unit]	Offset [mm]	Gelatine concentration [% wt]	Velocity [mm/s]
Circular	3	3	**4**
Diagonal	**10**	**8**	8
Two-by-two	20	13	13.5

Note. The baseline condition is annotated in bold.

Force experiment. Gelatine samples were prepared one day in advance of the experiment. A drilling spot along the edge of the gelatine container at least 30 mm apart from other drillings and from the edge of the container was chosen and the needle was positioned 1 mm above the gelatine. The waiting time between needle insertion and retraction was set to 3 s, to allow the gelatine around the needle to settle.

All force measurements were performed over a time span of one day. Needle velocity (4, 8, and 13.5 mm/s) and gelatine concentration (3, 8, and 13% wt) were varied in a fully crossed manner. Each combination of parameters was repeated five times. Temperature of the gelatine was kept between 4 and 8 C^o in both experiments, as the insertion force of a needle in gelatine decreases for temperatures above 8^{o}C [28].

4.4 Data processing

Prototype experiment. The raw signal of the cart position was filtered using a moving average filter over five samples. S_a was calculated by subtracting the mean value of the last 10 data samples from the first 10 data samples. N_c was determined by the number of local maxima in the signal. $Slip_{pro}$ was determined by subtracting the cart position after the protrusion phase of a given cycle from the cart position before the

protrusion phase of the cycle. $Slip_{ret}$ was determined by subtracting the difference in cart position before and after the retraction phase from the offset.

Force experiment. The raw force signal was filtered using a moving average filter over 100 samples and shifted so that the first 1,000 data points (i.e., 1 s) averaged at zero. The retraction phase was defined as the part of the curve from maximum retraction to substrate exit. The protrusion phase was defined as the part of the curve until maximum protrusion, with the same length as the retraction part. The protrusion and retraction force profiles were aligned at their maximum force value. The resultant of the retraction and protrusion force is the cutting force. The depth at which cutting and friction forces were in equilibrium (Eq. 1) was determined by the intersection between a linearly fitted retraction force and the mean cutting force.

4.5 Statistical analysis

For the prototype experiment, a one-way ANOVA was performed to compare the means of SR_{pro}, SR_{ret}, and SR_{tot} as a function of the parameters in **Table 1**. For the force experiment, a one-way ANOVA was performed to compare the means of the maximum friction and average cutting force as a function of needle velocity and gelatine concentration. Data analysis was performed in MATLAB R2013a (The MathWorks, Inc., Natick, Massachusetts).

5 Results

5.1 Prototype experiment

SR_{tot} was not significantly different between circular and diagonal actuation in 8% wt gelatine at 4 mm/s ($F(1,8) = 0.56$, $p = .476$; **Fig. 3**). Two-by-two actuation of needle parts resulted in no penetration at 4 mm/s and in penetration with a SR_{tot} higher than 0.9 at 13.5 mm/s. A 4-mm offset was associated with a higher SR_{tot} as compared to SR_{tot} for 10-mm and 20-mm offsets ($F(2,12) = 160.54$, $p < .001$; the latter two also being significantly different from each other; post-hoc paired *t*-test: $p = .009$). SR_{tot} increased with gelatine concentration ($F(2,12) = 154.71$, $p = 2.70.10^{-9}$). SR_{tot} did not differ between the three tested velocities ($F(2,12) = 1.43$, $p = .278$). SR_{pro} decreased with offset and increased with gelatine concentration, in line with the effects observed for SR_{tot}, whereas SR_{ret} decreased with offset and gelatine concentration.

5.2 Force experiment

The maximum friction force increased with needle velocity for all three gelatine concentrations (3% wt: $F(2,12) = 17.6$, $p < .001$; 8% wt: $F(2,12) = 10.33$, $p = .003$; 13% wt: $F(2,12) = 47.83$, $p < .001$). Also the average cutting force increased with needle velocity (3% wt: $F(2,12) = 40.62$, $p < .001$; 8% wt: $F(2,12) = 131.3$, $p < .001$; 13%

wt: F(2,12) = 50.91, $p < .001$). The equilibrium depth increased with velocity and decreased with gelatine concentration.

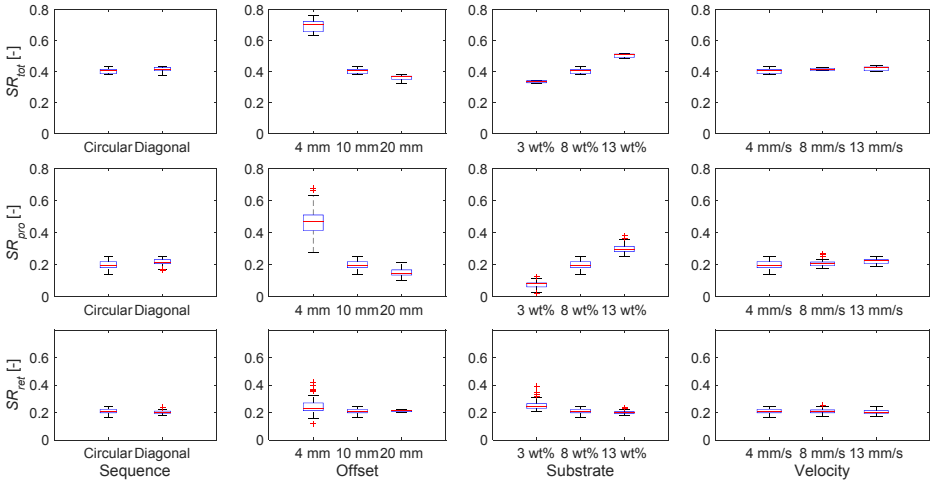

Fig. 3. Prototype experiment. Slip ratio as a function of each of the independent variables (from left to right: sequence, offset, gelatine concentration, velocity) (top row) per cycle (SR_{tot}); (middle row) in the protrusion phase (SR_{pro}); and (bottom row) in the retraction phase (SR_{ret}).

6 Discussion

We tested the principle of needle advancement through tissue phantom material with low net push force while using a four-part needle devoid of surface gripping textures. We found that slip ratio decreased with decreasing gelatine concentration and increasing offset. Friction force increased with velocity, gelatine concentration, and penetration depth, whereas cutting force increased with velocity and gelatine concentration, and remained constant with penetration depth.

6.1 Main findings

Gelatine concentration. We found a proportional relation between SR_{tot} and gelatine concentration, which is not in line with our hypothesis and Eq. 1 but is consistent with Parittotokkaporn et al. (2009) who reported substrate traversal with slip in 6% wt gelatine and no substrate traversal at all in 8% wt gelatine. A parameter possibly contributing to the observed proportional relation is the elastic deformation of the gelatine: when all four needle parts are protruded, the cart moves slightly backwards due to the gelatine springing back. It is possible that this effect increases with gelatine concentration, as friction increases with gelatine concentration more than elasticity does [29–31]. Cart inertia and bearing friction possibly also contribute to the observed proportional relation between SR_{tot} and gelatine concentration. Specifically, the resistance against movement of the cart may act as a pushing force on the protruding

needle part, preventing the cart from moving backwards. Cutting force increases with gelatine concentration (in line with [25,28,30]), leaving us to believe that the effect of cart inertia and bearing friction on $Slip_{\mathrm{pro}}$ decreases with gelatine concentration.

Offset. Whereas the absolute amount of slip *per cycle* was proportional to the offset in agreement with our hypothesis, the total amount of slip decreased with offset, meaning that the best overall performance was achieved with the largest offset. The elastic deformation described in the previous paragraph could contribute to the relatively high SR_{tot} for small offsets. As the absolute effect of elasticity should be equal for the three offsets, the relative contribution to the SR_{pro} is higher for small offsets. This is supported by an exploratory test with an offset of 1 mm, which resulted in no penetration at all, possibly because in that case only elastic deformation was achieved.

Sequence. No performance difference between one-by-one circular and diagonal actuation was found, which is expected, as the surface area subjected to resistive forces is independent from the actuation order of the needle parts. Two-by-two actuation yielded no penetration at 4 mm/s, suggesting that the difference in friction between protruding and stationary needle parts is the dominant factor for needle penetration. Two-by-two actuation at 13.5 mm/s resulted in penetration with a slip ratio over 0.9, probably due to cart inertia: due to the relatively large mass of the cart, the protruding needle part accelerated forwards faster than the cart was able to accelerate backwards.

Velocity. No slip reduction was observed for increasing needle-part velocity, contradicting our hypothesis. Force measurements indicated that the cutting force increased more steeply with needle velocity than the friction force did, opposite to [25]. The difference in maximum acceleration for different velocities in the prototype experiment makes the validation of the performance results difficult. Future experiments with varying velocity require a trade-off between maximum acceleration and acceleration time to reach a certain needle-part velocity, as a reduction of acceleration results in a longer acceleration time, whereas for high acceleration differences between velocity settings, inertia confounds the effect of velocity on performance.

6.2 Limitations

Cart inertia and bearing friction possibly prevented slip in the protrusion phase in which the resultant force on the cart was directed out of the gelatine. The cart weighed 0.73 kg and accelerated with a maximum of 27 mm/s^2 in the 4-mm/s velocity setting, therefore requiring a force of about 0.02 N to overcome its inertia. To overcome bearing friction, a force of about 0.015 N would be needed (assuming a friction coefficient of 0.002 for lubricated ball bearings; [32]). Thus, in the protrusion phase, where the resultant force on the needle is likely to be lower than 0.035 N, an effect of inertia and bearing friction cannot be ruled out.

To validate the method used to define friction and cutting force, supplementary measurements were conducted, in which friction force was measured when the entire needle was inserted 5 times in the same hole in 3%, 8%, and 13% wt gelatine. Results

showed that in all three concentrations the retraction force declined after the first insertion by about 10%. These results indicate that friction force both in our force experiments and in the literature is generally underestimated and therefore the cutting force is overestimated, due to the fact that the retraction (thereby friction) force is measured *after* the hole is already made during the insertion movement of the needle.

In this work, we only focused on straight trajectories. Frasson et al. [7] showed that steering with a multipart needle can be achieved by controlling the relative offset between needle parts. Asymmetric forces acting from the substrate on the (bevelled) tip cause the needle to cut a curved trajectory. Wasps are also capable of bending their ovipositors in several ways (e.g., [33]). Further research is required to find the most suitable way of steering a multipart needle.

Acknowledgements. This research is supported by the Dutch Technology Foundation STW, which is part of the Netherlands Organization for Scientific Research (NWO), and which is partly funded by the Ministry of Economic Affairs (project 12712, STW Perspectief Program iMIT-Instruments for Minimally Invasive Techniques).

References

1. Abolhassani, N., Patel, R., Moallem, M.: Needle Insertion into Soft Tissue: A Survey. Med. Eng. Physics 29, 413–431 (2007)
2. Misra, S., Reed, K.B., Schafer, B.W., Ramesh, K.T., Okamura, A.M.: Observations and Models for Needle-Tissue Interactions. IEEE Int. Conf. on Robotics and Automation, pp. 2687–2692 (2009)
3. Frasson, L., Parittotokkaporn, T., Davies, B.L., Rodriguez y Baena, F.: Early Developments of a Novel Smart Actuator Inspired by Nature. 15th Int. Conf. on Mechatronics and Machine Vision in Practice, pp. 163–168 (2008)
4. Ebrahimi, R., Okazawa, S., Rohling, R., Salcudean, S.E.: Hand-Held Steerable Needle Device. In: Ellis, R.E., Peters, T.M. (eds.) Medical Image Computing and Computer-Assisted Intervention – MICCAI 2003, pp. 223–230 (2003)
5. Engh, J.A., Podnar, G., Khoo, S.Y., Riviere, C.N.: Flexible Needle Steering System for Percutaneous Access to Deep Zones of the Brain. IEEE 32nd Annu. Northeast Conf. on Bioengineering, pp. 103–104 (2006)
6. Frasson, L., Ko, S.Y., Turner, A., Parittotokkaporn, T., Vincent, J.F., Rodriguez y Baena, F.: STING: A Soft-Tissue Intervention and Neurosurgical Guide to Access Deep Brain Lesions Through Curved Trajectories. J. Eng. Med. 224, 775–788 (2010)
7. Frasson, L., Ferroni, F., Ko, S.Y., Dogangil, G., Rodriguez y Baena, F.: Experimental Evaluation of a Novel Steerable Probe With a Programmable Bevel Tip Inspired by Nature. J. Robot. Surg. 6, 189–197 (2012)
8. Walsh, C.J., Franklin, J.C., Slocum, A., Gupta, R.: Material Selection and Force Requirements for the Use of Pre Curved Needles in Distal Tip Manipulation Mechanisms. Design of Medical Devices Conference, 3913 (2010)
9. Webster, R.J., Okamura, A.M., Cowan, N.J.: Toward Active Cannulas: Miniature Snake-Like Surgical Robots. IEEE/RSJ Int. Conf. on Intelligent Robots and Systems, pp. 2857–2863 (2006)
10. Scali, M., Pusch, T.P., Breedveld, P., Dodou, D.: Needle-Like Instruments for Steering Through Solid Organs: a Review of the Scientific and Patent Literature (submitted)

11. Van de Berg, N.J., Van Gerwen, D.J., Dankelman, J., Van den Dobbelsteen, J.J.: Design Choices in Needle Steering—A Review. IEEE-ASME T. Mech. 20, 2172–2183 (2015)
12. Rahman, M.H., Fitton, M.G., Quicke, D.L.: Ovipositor Internal Microsculpture in the Braconidae (Insecta, Hymenoptera). Zool. Scr. 27, 319–332 (1998)
13. Scudder, G.G.E.: Comparative Morphology of Insect Genitalia. Annu. Rev. Entomol. 16, 379–406 (1971)
14. Vincent, J.F.V., King, M.J.: The Mechanism of Drilling by Wood Wasp Ovipositors. Biomimetics 3, 187–201 (1995)
15. Burrows, C., Secoli, R., Rodriguez y Baena, F.: Experimental Characterisation of a Biologically Inspired 3D Steering Needle. 13th IEEE Int. Conf. on Control, Automation and Systems, pp. 1252–1257 (2013)
16. Frasson, L., Parittotokkaporn, T., Schneider, A., ... Rodriguez y Baena, F.R.: Biologically Inspired Microtexturing: Investigation into the Surface Topography of Next-Generation Neurosurgical Probes. 30th IEEE Annu. Int. Conf. of the Engineering in Medicine and Biology Society, pp. 5611–5614 (2008)
17. Leibinger, A., Oldfield, M., Rodriguez y Baena, F.R.: Multi-Objective Design Optimization for a Steerable Needle for Soft Tissue Surgery. 15th Int. Conf. on Biomedical Engineering, pp. 420–423 (2014)
18. Oldfield, M.J., Burrows, C., Kerl, J., Frasson, L., Parittotokkaporn, T., Beyrau, F., Rodriguez y Baena, F.: Highly Resolved Strain Imaging During Needle Insertion: Results With a Novel Biologically Inspired Device. J. Mech Beh. Biomed. Mat. 30, 50–60 (2014)
19. Parittotokkaporn, T., Frasson, L., Schneider, A., ... Rodriguez y Baena, F.R.: Soft Tissue Traversal with Zero Net Push Force: Feasibility Study of a Biologically Inspired Design Based on Reciprocal Motion. IEEE Int. Conf. on Robotics and Biomimetics, pp. 80–85 (2009)
20. Aoyagi, S., Takaoki, Y., Takayanagi, H., ... Matsumoto, T.: Equivalent Negative Stiffness Mechanism Using Three Bundled Needles Inspired by Mosquito for Achieving Easy Insertion. 2012 IEEE/RSJ Int. Conf. on Intelligent Robots and Systems, pp. 2295–2300 (2012)
21. Sakes, A., Dodou, D., Breedveld, P.: Buckling Prevention Strategies in Nature as Inspiration for Improving Percutaneous Instruments: A Review. Bioinsp. Biomim. 11 (2016), pp. 021001-1–021001-26.
22. Syringe Needle Gauge Chart, http://www.sigmaaldrich.com/chemistry/stock room-reagents/learning-center/technical-library/needle-gauge-chart.html (2014
23. Hing, J.T., Brooks, A.D., Desai, J.P.: Reality-Based Needle Insertion Simulation for Haptic Feedback in Prostate Brachytherapy. IEEE Int. Conf. on Robotics and Automation, pp. 619–624 (2006)
24. Simone, C., Okamura, A.M.: Modeling of Needle Insertion Forces for Robot-Assisted Percutaneous Therapy. IEEE Int. Conf. on Robotics and Automation, 2, 2085–2091 (2002)
25. Van Gerwen, D.J., Dankelman, J., Van den Dobbelsteen, J.J.: Needle-Tissue Interaction Forces-A Survey of Experimental Data. Med. Eng. Phys. 34, 665–680 (2012)
26. Nguyen, M.M., Zhou, S., Robert, J.L., Shamdasani, V., Xie, H.: Development of Oil-In-Gelatin Phantoms for Viscoelasticity Measurement in Ultrasound Shear Wave Elastography. Ultrasound Med. Biol. 40, 168–176 (2014)
27. Moreira, P., Peterlik, I., Herink, M., Duriez, C., Cotin, S., Misra, S.: Modelling Prostate Deformation: SOFA Versus Experiments. Mech. Eng. Res. 3, 64–72 (2013)
28. Ng, K.W., Goh, J.Q., Foo, S.L., Ting, P.H., Lee, T.K.: Needle Insertion Forces Studies for Optimal Surgical Modeling. Int. J. Bioscience Biochem. Bioinformatics, 3, 187–191 (2013)

29. Zhang, X., Qiang, B., Greenleaf, J.: Comparison of the Surface Wave Method and the Indentation Method for Measuring the Elasticity of Gelatine Phantoms of Different Concentrations. Ultrasonics 51, 157–164 (2011)
30. De Lorenzo, D.: Force Sensing and Display in Robotic Driven Needles for Minimally Invasive Surgery. Doctoral dissertation, Politecnico di Milano, Milano (2012)
31. Crouch, J.R., Schneider, C.M., Wainer, J., Okamura, A.M.: A Velocity-Dependent Model for Needle Insertion in Soft Tissue. In: Duncan, J.S., Gerig, G. (eds.) Medical Image Computing and Computer-Assisted Intervention – MICCAI 2005, pp. 624–632 (2005)
32. Van Beek, A.: Advanced Engineering Design: Lifetime Performance and Reliability. Delft University of Technology, Delft (2006)
33. Quicke, D.L.: Ovipositor Mechanics of the Braconine Wasp Genus Zaglyptogastra and the Ichneumonid Genus Pristomerus. J. Natural History 25, 971–977 (1991)